Experimental Validation of 1D model for photovoltaic/ thermal (PV/T) modules

Laetitia Brottier[1,3], David Cheze[2], Mathieu Mariotto[2], Franck Medlege[2], Guillaume Razongles[2] and Rachid Bennacer[3]

[1] DualSun, Marseille (France)

[2] CEA, Le Bourget-du-Lac (France)

[3] LMT/ENS-Cachan/CNRS/Université Paris Saclay, Cachan (France)

Abstract

To understand specific performance characteristics of a flat photovoltaic thermal (PV/T) module, a general simplified model (1D) has been performed, leading to an exponential equation for output temperature when weather and input fluid characteristics are known. To validate the model, a unique parametrical experimental validation was performed and is the focus of this paper. The present work includes nine prototypes built and monitored with the normative Solar Keymark approach.

The model exhibit a good fit with the experimental results. This conclusion has to be confirmed for future prototypes based on a polymeric heat exchanger.

Keywords: Photovoltaic thermal (PV/T) collector; Experimental validation; Energy performance

1. PV/T context and propose of the work

Since 2015, solar power is the number one energy source in terms of new capacities of electricity production ahead of coal, and the IEA published in Renewable 2017 (Renewable 2017, IEA) that the share of renewables for electrical needs will be 30% in 2022.

UNEP estimates that the buildings sector represent 30% of total energy consumption in the world (Global Status Report 2016, UNEP). Photovoltaics (PV) on buildings is ineluctable and the European Energy Performance of Buildings Directive requires all new buildings to be Nearly Zero-Energy (NZEBs) by the end of 2020. This directive is one of the political initiatives that gives a frame for its massive development.

But heat will certainly be the issue of the 21st century for Buildings. Almost 80% of energy demand in the buildings sector is for heat according to the IEA's article (Renewable energy's next frontier: heat, 6/12/2016).

Even with a strongly insulated building, the need for domestic hot water (DHW) is still here, and the space on the buildings' rooftops is not infinite. That is why the "2-in-1" PV/T technology a key solution to meeting energy needs of highly energy-efficient buildings. PV/T modules enable to produce DHW and photovoltaic with the same module, and make buildings more and more autonomous in heat and electricity using solar power.

Additionally, building-integrated PV (BIPV) may lead to a decrease in electrical performance of photovoltaic cells due to an increase in operating cell temperature (0.5%/K for mono-crystalline technology). In this context, the design of hybrid Photovoltaic-Thermal (PV-T) collectors, which recover wasted heat from the photovoltaic panel and in effect reduce cell temperature, offer an innovative solution for BIPV.

A review of PV/T technologies has been done by Zhang *et al.* (2012) and Good *et al.* (2015). The DualSun PV/T module in the study (Fig. 1) is based on the unglazed flat-plate liquid design described in these reviews. It has 60 monocrystalline cells for a nominal power of 250 Wp (PV) and 912Wth (Thermal).

doi:10.18086/swc.2017.18.04 Available at http://proceedings.ises.org

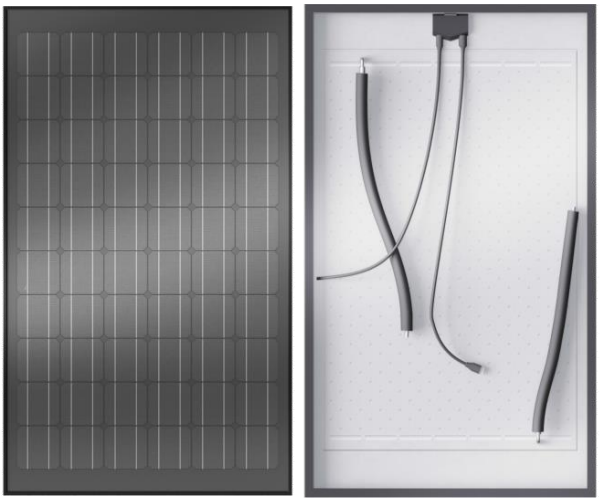

Fig. 1: DualSun PV/T module, 60 cells 250Wp, direct lamination of a stainless steel heat exchanger 912Wth

As reported by Zondag, H.A., 2008 in his review on flat-plate PV-T collectors, one key point for the development of PV-T collectors concerns the heat transfer between PV cells and fluid. That is why DualSun focused during their PV/T module developments on heat transfer between PV cells and fluid. Thermal resistance has been minimized by direct lamination of the specific heat exchanger. Direct lamination is possible due to a pertinent material choice, which prevents delamination due to differential dilatation in the long term.

As Dupeyrat, P., et al., 2009 pointed out, glazed PV-T modules lead to a better overall energy conversion. But DualSun has made the choice of an unglazed collector to keep a low stagnation temperature, and thus prevent overheating. The PV encapsulant is very sensitive to high temperature, which could irreversibly destruct the laminate. Furthermore, the residential sector, stagnation will often occur during summer months when families have left on vacation, and thus when solar irradiation is important.

The original concept of the DualSun module is different from what can be observed in existing literature. In order to simulate the energetic performances of the DualSun module, a numerical 1D model was developed. To validate the 1D model, the layers of the module have been changed in this study and tested.

2. Numerical model

An energy balance of the module leads to a quasi 1D simplified model, a methodology which has been previously used by many authors (Chow et al. 2008, Duffie and Beckman 1991, Fraisse et al. 2017, Tess library). The model input values include weather entries (ambient temperature T_A, insulation, wind velocity V_{WIND}) and solar domestic hot water load parameters (stock bottom temperature $T_{F,IN}$, flow rate $\dot{m}$). Thanks to an energy balance (Fig.2) on photovoltaic cells and on a fluid slice (eq. 1), we deduce an exponential behavior of fluid temperature along the path (eq. 2).

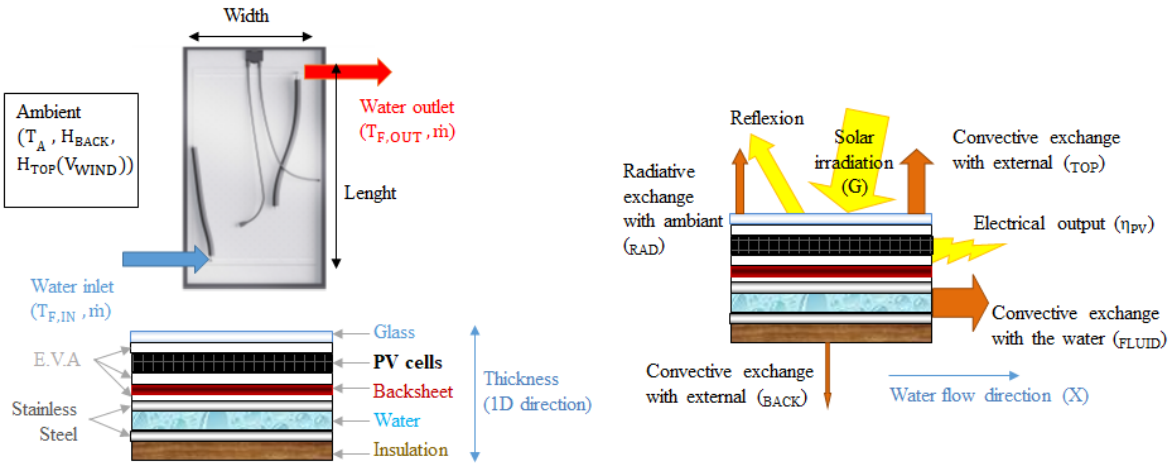

Fig. 2: Description of the studied system

Module output temperature and electrical power are then deduced thanks to an iterative approach on photovoltaic temperature (T_{PV}). The definitions of the symbols are given in Tab. 1 and subscript in Tab. 2.

$$\underbrace{(\tau_\alpha).G.\left(1-\eta_{PV}(G,T_{PV})\right)}_{Solar\ Recovered\ energy} = \underbrace{h_{RAD}(T_{PV}).(T_{PV}(x)-T_{SKY})}_{Radiative\ exchange\ with\ ambiant} + \underbrace{H_{TOP}(V_{WIND}).(T_{PV}(x)-T_A)}_{Convective\ exchange\ with\ external} + \underbrace{H_{FLUID}.\left(T_{PV}(x)-T_F(x)\right)}_{Convective\ exchange\ with\ the\ water} \quad \text{(eq.1)}$$

$$\underbrace{H_{FLUID}.\left(T_{PV}(x)-T_F(x)\right)}_{Convective\ exchange\ with\ the\ water} = \underbrace{H_{BACK}.(T_F(x)-T_{BACK})}_{Convective\ exchange\ with\ external} + \dot{m}.Cp.\frac{dT_F}{dx} \quad \text{(eq.2)}$$

Module outlet temperature and electrical power are then deduced thanks to an iterative approach on photovoltaic temperature (T_{PV}).

$$T_{F,OUT} = \left(T_{F,IN} - C\right).\ e^{-D.Width} + C \quad \text{(eq.3)}$$

$$T_{PV} = A\ .\ T_{F,MEAN} + B \quad \text{(eq.4)}$$

In non-null flow rate cases, equations were simplified to follow Solar Keymark standard directives (eq. 5).

$$\eta_{TH} = a_0 - a_1\ .\left(\frac{T_{F,MEAN}-T_A}{G}\right) \quad \text{(eq.5)}$$

Relations between the 1D-model and the linear formula are given by Eqs. 6 and 7.

$$a_0 = \frac{\dot{m}\cdot Cp\cdot D\cdot Width\cdot(C-T_A)}{G\cdot Area} \quad \text{(eq. 6)}$$

$$a_1 = \frac{\dot{m}\cdot Cp\cdot D\cdot Width}{Area} \quad \text{(eq. 7)}$$

Tab. 1: Meaning and units for symbols

Symbol	Meaning	Units
A,B,C and D	Coefficients depending on module characteristics	
Cp	Heat capacity	W/kg/K
G	Solar irradiation	W/m²
H	Global coefficient	W/m²/K
h_{RAD}	Radiative coefficient	W/m²/K
H_{WIND}	Convective coefficient on top plate due to the wind	W/m²/K
H_{FLUID}	Convective coefficient on the plate due to the water	W/m²/K
$\dot{m}$	Water Flow rate	L/s
T	Temperature	K
V_{WIND}	Wind velocity	m/s
Width	Width of solar collector	m
X	Water flow direction	
Tα	Transmitto-absorption depending on diffuse, direct and horizontal irradiation	-
η_{PV}	Electrical efficiency	-
η_{TH}	Thermal efficiency	-

Tab. 2: Meaning for subscripts

Subscript	Meaning
A	Ambient
BACK	Between fluid and back ambient
F	Fluid
FLUID	Between PV cells and fluid
PV	Photovoltaic cells
TOP	Between cells and ambient

3. Prototypes and testing

Some experimental validations at the module level were proposed but only with specific heat exchanger (Ben Cheikh et al. 2015, Rejeb et al. 2016). The aim of this paper is to do a complete parametric validation with a basic shape for the integrated heat exchanger with a full water slice (no tubes).

In order to validate the proposed simplified model, 9 prototypes were build and monitored according to the Solar Keymark approach in a sunlight test bench. All prototypes size 1669 x 982mm², except n°8 and 9, which were smaller (1365 x 886mm²). All integrated heat exchangers are directly laminated with the cells with an Ethylene Vinyl Acetate layer (EVA) under the BackSheet (BS) during a unique lamination step. Such manufactured heat exchanger (0.6mm stainless steel plates) allow a 2mm water gap to cool the photovoltaic part and have a 15mm non-irrigated border.

The description of the constitutive layers for the 9 prototypes tested are summarized in Tab. 3.

Tab. 3: description of the 9 prototypes tested

	Glass (mm)	EVA (mm)	Cells	EVA (mm)	BS (mm)	Fixation (mm)	Stainless Steel Heat exchanger / PV surface	Insulation equivalent thickness (k=0.033 W/(m.K))
1	2	0.6	60 (MPPT)	1.2	0.4	1.2	74%	NO
2	2	0.6	60 (OC)	1.2	0.4	1.2	74%	NO
3	2	0.6	60 (MPPT)	1.2	0.4	1.2	74%	39.6mm
4	2	0.6	60 (MPPT)	1.2	0.4	1.2	74%	24.8mm
5	2	0.6	60 (MPPT)	0.6	0.4	0.6	74%	NO
6	4 Low E	0.6	60 (MPPT)	1.2	0.4	1.2	74%	NO
7	2	-	-	0.6	0.4	0.6	74%	NO
8	-	-	-	-	-	-	exch only	NO
9	2	0.6	40 (OC)	1.2	0.4	1.2	100%	NO

The bench of artificial sunlight consists of two independent parts: the lamp holder and the sensor holder. The simulator is class BBB (Fig. 2). For the characterization of the PV/T module, an irradiant flux of 1000W / m² is adjusted at the level of the lamps.

Fig. 2: Pictures of the artificial sunlight test bench

A mapping of the flux measurements is carried out in order to check a homogeneity on the surface of the sensor of plus or minus 5% on the mean value of the flux (Fig. 3). This mapping is carried out with each new characterization and it is obvious that the flux homogeneity is within ±1.5%.

Height [mm]	G = Irradiation [W/m²] - Average = 1006.36W/m²							
1590	942,0	956,4	960,4	971,0	964,1	961,1	962,6	944,0
1440	974,7	986,8	988,3	997,3	985,5	982,8	986,2	96 ,5
1290	998,9	1006,4	1006,7	1010,7	997,7	993,6	997,5	98 ,0
1140	1036,9	1046,7	1041,6	1038,3	1026,8	1021,7	1021,1	10 0,4
990	1044,8	1056,7	1053,5	1056,5	1040,8	1035,6	1039,9	10 1,2
840	1049,9	1061,3	1061,3	1063,5	1050,3	1047,0	1048,7	10 0,2
690	1044,9	1056,1	1056,9	1059,5	1049,6	1045,9	1048,4	10 9,2
540	1017,0	1031,2	1032,7	1037,4	1029,6	1027,9	1029,2	10 1,8
390	9 ,9	997,7	997,3	1003,6	996,9	996,9	998,6	98 ,0
240	980,8	993,4	991,5	991,1	988,4	986,3	987,8	97 ,9
90	972,1	977,9	980,6	984,3	974,7	976,0	981,3	96 ,4
-60	970,9	976,5	978,1	984,3	974,7	974,6	980,1	962,9
Width [mm]	-700	-550	-400	-250	-100	50	200	350

Fig. 3: Mapping measurements of the irradiation [W/m²]

Fans are used to generate a wind parallel to the top of the analysed system. A mapping of the air flow velocity measurements is carried out by means of a mobile hot wire sensor (Fig. 4). A speed around 1.5m / s is targeted.

Height [mm]	Air speed [m/s] - Average = 1.63m/s							
1590	1,12	1,35	1,45	1,48	1,63	1,61	1,50	1,34
1440	1,26	1,42	1,40	1,64	1,62	1,70	1,44	1,48
1290	1,46	1,43	1,52	1,64	1,57	1,73	1,67	1,39
1140	1,30	1,40	1,53	1,57	1,65	1,68	1,77	1,39
990	1,28	1,53	1,61	1,76	1,77	1,62	1,71	1,39
840	1,38	1,34	1,62	1,60	1,70	1,62	1,74	1,43
690	1,05	1,62	1,74	1,68	1,61	1,66	1,66	1,39
540	1,41	1,64	1,63	1,85	1,88	1,79	1,69	1,59
390	1,44	1,61	1,71	1,85	1,83	1,75	1,73	1,51
240	1,89	1,76	1,76	1,73	1,82	1,91	1,78	1,53
90	1,83	1,94	1,87	1,89	1,73	2,02	1,84	1,47
-60	2,00	2,00	1,95	2,00	1,69	1,90	1,97	1,46
Width [mm]	-700	-550	-400	-250	-100	50	200	350

Fig. 4: Mapping measurements of the wind speed [m/s]

A thermal regulation ensures the conditioning of the fluid (water), in order to generate a regulated inlet temperature in the module and to ensure good circulation in the exchanger. Six input temperature steps from 20 ° C to 70 ° C are programmed to scan the operating range of the module.

Local input / output temperature measurements and fluid flow measurements make it possible to draw up the appropriate thermal balances and determine the powers involved for each thermally stabilized operating point.

The measuring instrument I (V) plots the curves and extracts the important photovoltaic values. The red rectangle shows the location of the reference cell for the instrument which plots the I (V) curves, and the blue rectangle the module location (Fig. 3). The power of the module is limited by the current of the least photo-generating cell, which depends mainly on the minimum irradiance that the surface of the module receives (the limiting cell). In practice, the power value "equivalent to 1000 W / m²" is obtained from the reference cell (approx. -5% deviation).

Results are given in Tab.4.

Tab. 4: Thermal and photovoltaic results for the 9 prototypes

	a_0 (%)	a_1 (W/K/m²)	Wp *	β (%/°C)
1	50.2	12.8	238	-0.048
2	59.9	13.1	-	-
3	49.6	10.6	238	-0.050
4	49.8	11.4	238	-0.050
5	52.8	13.1	245	-0.055
6	49.8	13.0	225	-0.050
7	66.1	13.3	-	-
8	39.8	11.3	-	-
9	75.7	17.9	-	-

*limiting cell equivalent power at 1000W/m² and 25°C

4. Model validation

Two parameters were introduced to take better into account for the specific behavior of the Dualsun stainless steel heat exchanger. The first was the ratio Stainless Steel Heat exchanger over PV surface for the effect of the fin. Additionally, the heat exchange between the fluid and the stainless steel was supposed fixed at 800 W/(m².K) but is unknown. The second parameter was length of exchange.

Both parameter have been deduced from numerical optimization. The ratio Stainless Steel Heat exchanger over PV surface has been raised from a numerical optimization to 82% instead of 74%. The length of exchange has been optimized to fit with the experimental results to 770mm instead of 856mm.The model fit the experimental data very well as shown in Tab. 5 and Fig. 5 with a maximum root-mean-square error (RMSE) inferior of 67 to compare with the 1000Wth. The quality of the direct lamination for the 9th prototype was harder to achieve with the unusual size, which certainly explains the higher error with the theory.

These results seems to confirm that the 3D design could be neglect to predict performances, but this analyze could not be directly use for non-conductive material for the heat exchanger, as it could be an effect of the high homogenization of the temperature in the heat exchanger due to the relatively high conduction in the stainless steel. So it would be interested to continue this study with a polymeric heat exchanger.

Tab. 5: Root-mean-square error for each model/ test fitting

Test	1	2	3	4	5	6	7	8	9
RMSE	8.74	17.14	26.39	15.09	29.98	20.33	28.35	25.42	66.98

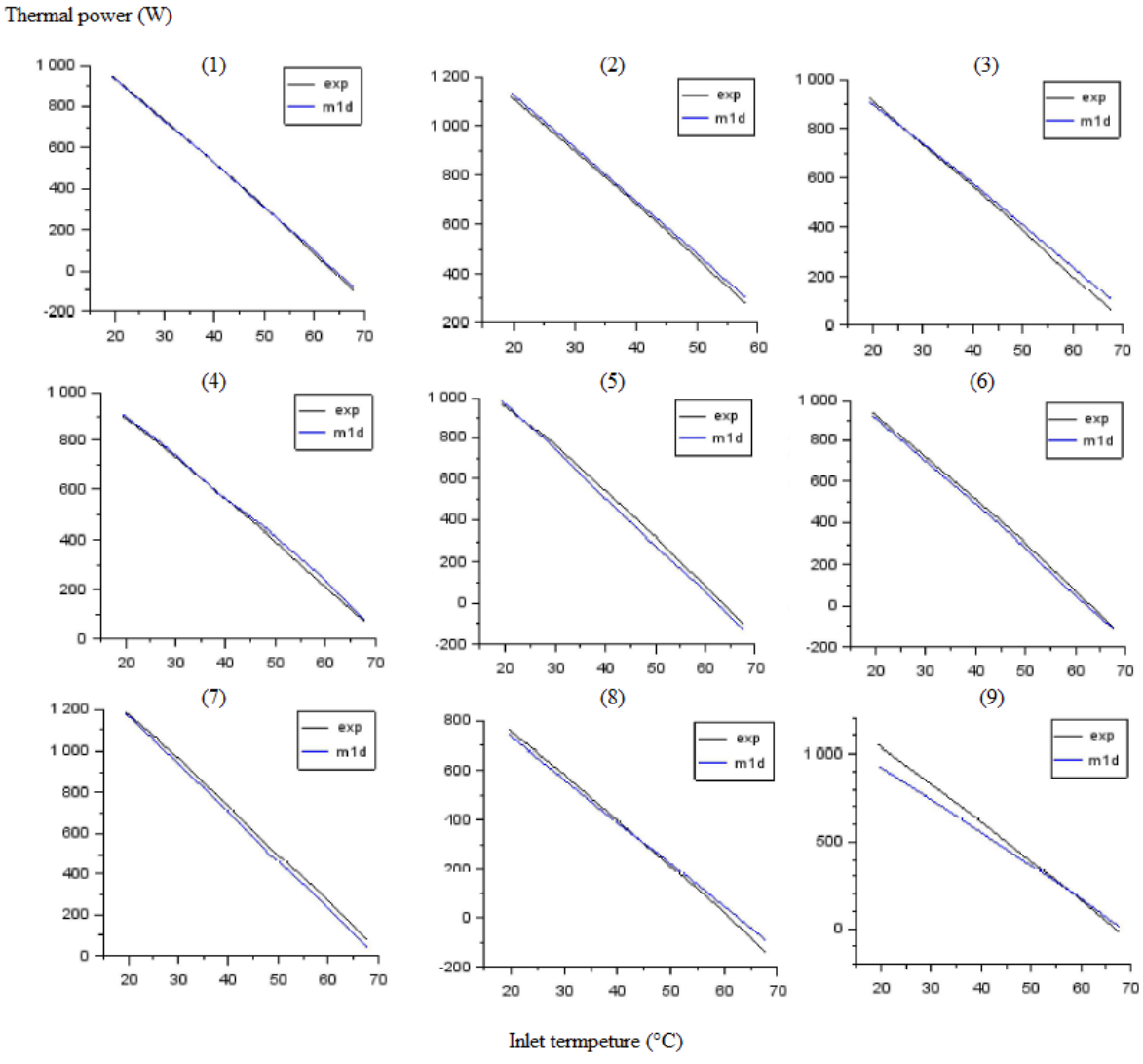

Fig. 5: Experimental and theorical thermal performance curves for the 9 prototypes

5. Conclusion

In this study, a general simplified model (1D) of PV/T module was proposed leading to an exponential equation for output temperature when weather and input fluid characteristics are known.

To challenge this model, the layers properties have been changed in 9 prototypes. The electrical and thermal performances of these 9 prototypes has been experimentally monitored with the normative Solar Keymark approach, and then compared with the performance outputs of the model.

The 9 first prototypes performance results have a good fit with the 1D model. These encouraging results must be confirmed with further tests with a polymeric heat exchanger.

6. References

Ben Cheikh El Hocine, et al., 2015, Model Validation of an Empirical Photovoltaic Thermal (PV/T) Collector, Energy Procedia. 74. 1090-1099

Chow, T.T., et al., 2008, Computer modeling and experimental validation of a building-integrated photovoltaic and water heating system, Applied Thermal Engineering 28, 1356–1364

Duffie, J.A., Beckman, W.A., 1991. Solar Engineering of Thermal Processes, second ed. Wiley Interscience, New York, 919p.

Dupeyrat, P., et al., 2009, International Scientific Conference - Renewables in a changing climate - From Nano to Urban Scale - CISBAT, Lausanne : Suisse

European Directive, Energy Performance of Buildings : 2010/31/UE, 19/05/2010

Fraisse, G., et al., 2007, Energy performance of water hybrid PV/T collectors applied to combisystems of Direct Solar Floor type. Solar Energy 81, 1426–1438

Good, C., et al., 2015. Hybrid photovoltaic-thermal systems in buildings – a review. Energy Procedia. 70, 683 – 690

IEA, Renewable 2017

IEA, Article, Renewable energy's next frontier: heat, 6/12/2016

Rejeb, O., et al., 2016, Numerical and model validation of uncovered nanofluid sheet and tube type photovoltaic thermal solar system, Energy Conversion and Management, 110. 367-377

Solar Keymark certification: http://www.estif.org/solarkeymarknew/index.php

TRNSYS - TESS libraries; library 17; TYPE 560: Fin Tube PV/T Solar Collector

UNEP, Global Status Report 2016

Zhang X., et al., 2012, Review of R&D progress and practical application of the solar photovoltaic/thermal (PV/T) technologies. Renewable and Sustainable Energy Reviews; Vol 16, Issue 1, p. 599–617

Zondag, H.A., 2008, Flat-plate PV-Thermal collectors and systems: A review. Renewable and Sustainable Energy Reviews. Volume 12, Issue 4, Pages 891-959.